Polarity Information Coded Flip-OFDM for Intensity Modulated Systems

Liang Wu, *Member, IEEE*, Zaichen Zhang, *Senior Member, IEEE*, Jian Dang, Jiangzhou Wang, *Senior Member, IEEE*, and Huaping Liu, *Senior Member, IEEE*

Abstract—A polarity-information-coded flip orthogonal frequency division multiplexing (PIC-flip-OFDM) is proposed for intensity modulation/direct detection (IM/DD) optical communications in this letter. In the proposed scheme, the modulated signals in the frequency domain are not constrained to have Hermitian symmetry. The real and imaginary parts of the time-domain complex signals are separated, and the polarities of the real and imaginary parts are jointly encoded and modulated. The transmit strategy and the receive algorithm of the proposed scheme are analyzed in detail. The major advantage of the proposed scheme is that its spectral and optical power efficiencies are higher than existing schemes, which is validated in simulation.

Index Terms—Intensity modulation/direct detection, polarity information coded, flip-OFDM.

I. INTRODUCTION

Orthogonal frequency division multiplexing (OFDM) was widely adopted in radio frequency (RF) communications because of its efficient use of spectrum and its ability to combat intersymbol interference (ISI) [1], [2]. In optical wireless communication systems with intensity modulation/direct detection (IM/DD), the transmitted signals are optical power, and thus must be real and non-negative. To meet these requirements, OFDM schemes have been modified for IM/DD optical communications [3]–[5]. Direct current biased optical OFDM (DCO-OFDM) is a straight-forward scheme by adding a DC offset to bipolar OFDM signals [3]. Asymmetrically clipped optical OFDM (ACO-OFDM) is another scheme, in which only the odd-indexed subcarriers are modulated and the negative signals are clipped to zero during transmission [4]. Pulse-amplitude-modulated discrete multitone (PAM-DMT) [5] and flip-OFDM [6] can achieve the same optical power and spectral efficiencies as ACO-OFDM. In the frequency domain, the modulated signals in these schemes must be Hermitian-symmetric to ensure that the time domain signals are real. The optical power efficiency of the DCO-OFDM scheme is lower than that of the ACO-OFDM scheme, because of the DC offset, which does not carry any information. The spectral efficiency of the DCO-OFDM scheme is the highest among
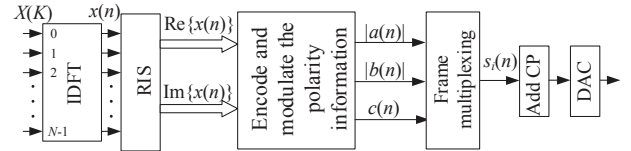
Fig. 1. Block diagram of the transmitter of the proposed PIC-flip-OFDM system (RIS denotes real and imaginary parts separation module and DAC is digital-to-analog converter).

these schemes assuming the same modulation order for the modulated subcarriers.

By employing coefficient separation [5], [7], a new flip-OFDM named polarity information coded flip-OFDM (PIC-flip-OFDM) is proposed in this letter. Since all subcarriers except the first and the middle ones can be modulated in the proposed PIC-flip-OFDM scheme, the modulated signals in the frequency domain are not Hermitian symmetric and the time-domain signal will be complex. The real and imaginary parts of the time-domain signal and their polarities are separated, and the polarities of real and imaginary parts are jointly encoded and modulated. The proposed PIC-flip-OFDM achieves a higher optical power efficiency than the DCO-OFDM scheme; compared with the traditional flip-OFDM or ACO-OFDM, the proposed PIC-flip-OFDM has a higher spectral efficiency; at a typical achievable spectral efficiency, the proposed PIC-flip-OFDM have the best performance.

II. TRANSMITTER OF THE PROPOSED PIC-FLIP-OFDM

Fig. 1 shows the block diagram of the transmitter of the proposed PIC-flip-OFDM. The output time-domain signal of the inverse discrete Fourier transform (IDFT) block can be expressed as

$$x(n) = \frac{1}{N} \sum_{K=0}^{N-1} X(K) e^{j\frac{2\pi}{N} Kn}, \quad n = 0, 1, \cdots, N-1, \quad (1)$$

where $X(K)$ with variance $\sigma_{X(K)}^2$ is the signal modulated on the K-th subcarrier, $j = \sqrt{-1}$, and N is the size of the IDFT. To avoid the DC shift, we set [6],

$$X(0) = X(N/2) = 0, \quad (2)$$

which means that no information will be modulated at the 0-th and the $(N/2)$-th subcarriers. In the proposed PIC-flip-OFDM, all subcarriers except two tones (the 0-th and the $(N/2)$-th subcarriers) could carry data, and the modulated signals in the frequency domain are not Hermitian symmetric. Therefore,

$x(n)$ is a complex bipolar signal with zero mean and variance σ_x^2 [8].

Define $a(n)$ and $b(n)$ as

$$\begin{cases} a(n) = \text{Re}\{x(n)\} \\ b(n) = \text{Im}\{x(n)\} \end{cases}, \tag{3}$$

where $\text{Re}\{\cdot\}$ and $\text{Im}\{\cdot\}$ denote the real part and the imaginary part of a complex number, respectively. The real and imaginary parts of $x(n)$ are real-valued random variables with zero mean and the same variance $\sigma_x^2/2$.

Define the polarities of the real and imaginary parts of $x(n)$ respectively as

$$\begin{cases} \text{sg}_{\text{Re}}(n) = \text{sign}\{a(n)\} \\ \text{sg}_{\text{Im}}(n) = \text{sign}\{b(n)\} \end{cases}, \tag{4}$$

where $\text{sign}\{\cdot\}$ is the sign function. From Eqs. (3) and (4), $x(n)$ can be expressed as

$$x(n) = \text{sg}_{\text{Re}}(n)|a(n)| + j\text{sg}_{\text{Im}}(n)|b(n)|, \tag{5}$$

where $|\cdot|$ denotes the absolute value, the electrical power of $|a(n)|$ or $|b(n)|$ is $\mathbb{E}[|a(n)|^2] = \mathbb{E}[|b(n)|^2] = \sigma_x^2/2$, and $\mathbb{E}[\cdot]$ stands for the expectation of a random variable.

The coding strategy for the polarities of $\text{Re}\{x(n)\}$ and $\text{Im}\{x(n)\}$ is listed in Table I, and the encoded output is defined as $d(n)$. When 4-ary unipolar pulse amplitude modulation (PAM) [9] is used to modulate the encoded polarity information, the modulator output is assumed to be $c(n)$. The electrical power of $c(n)$ is constrained to be

$$\mathbb{E}[c(n)^2] = \kappa\sigma_x^2, \tag{6}$$

where κ is a parameter that controls the power of $c(n)$.

After passing through the frame multiplexing module, $|a(n)|$, $|b(n)|$, and $c(n)$ consist of three different subframes as shown in Fig. 2. The sampling frequency of the proposed PIC-flip-OFDM is the same as that of DCO-OFDM. Therefore, the normalized bandwidths of the proposed PIC-flip-OFDM and DCO-OFDM are the same [8]. The bit rate/normalized bandwidth of the proposed PIC-flip-OFDM is expressed as

$$R_{\text{proposed}} = \frac{2}{3} \cdot \frac{2\sum\limits_{K=1,K\neq N/2}^{N-1} \log_2 M_K}{3(N_g + N)(1 + 2/N)} \quad \text{(bits/s/Hz)}, \tag{7}$$

where N_g is the length of cyclic prefix (CP), and M_K is the modulation order at the K-th subcarrier. When the modulation orders of all modulated subcarriers are the same and equal to M, the bit rate/normalized bandwidth of the proposed PIC-flip-OFDM is

$$R_{\text{proposed}} = \frac{2(N-2)\log_2(M)}{3(N_g + N)(1 + 2/N)} \quad \text{(bits/s/Hz)}, \tag{8}$$

TABLE I
CODING STRATEGY OF THE POLARITY INFORMATION

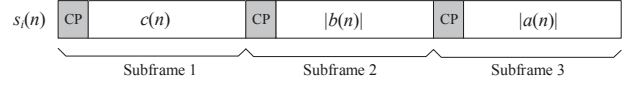| The sign of $a(n)$	The sign of $b(n)$	Encoded output (binary) $d(n)$
+	+	11
+	-	10
-	+	01
-	-	00

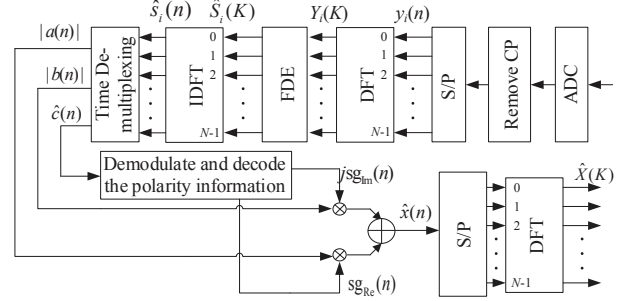Fig. 2. Frame structure of the proposed PIC-flip-OFDM.

Fig. 3. Block diagram of the receiver of the proposed PIC-flip-OFDM system.

while the bit rate/normalized bandwidth of the traditional flip-OFDM is [6]

$$R_{\text{flip-OFDM}} = \frac{(N/2 - 1)\log_2(M)}{(N_g + N)(1 + 2/N)} \quad \text{(bits/s/Hz)}. \tag{9}$$

Therefore, the proposed PIC-flip-OFDM achieves a higher spectral efficiency than the traditional flipped-OFDM when the same modulation order is employed.

III. RECEIVE ALGORITHM OF THE PROPOSED PIC-FLIP-OFDM

Fig. 3 shows the block diagram of the receiver of the proposed PIC-flip-OFDM. After removing CP, the i-th received subframe in the discrete-time domain can be expressed as

$$y_i(n) = h_i(n) \circledast s_i(n) + w_i(n), \tag{10}$$

where $h_i(n)$ is the impulse response of the IM/DD channel during the i-th subframe, $\circledast$ denotes cyclic convolution, $s_i(n)$ is the transmitted signal in the i-th subframe (Note that $s_1(n) = c(n)$ for the first subframe, $s_2(n) = |b(n)|$ for the second subframe, and $s_3(n) = |a(n)|$ for the third subframe), and $w_i(n)$ is the noise component with zero mean and variance σ_n^2. In a slowly changing environment, it is reasonable to assume that channel is constant over three consecutive OFDM subframes, that is, $h_1(n) = h_2(n) = h_3(n) = h(n)$, which is assumed in this letter.

In the frequency domain, the received signal is given by

$$Y_i(K) = H(K)S_i(K) + W_i(K) \tag{11}$$

where $Y_i(K) = \text{DFT}[y_i(n)]$, $S_i(K) = \text{DFT}[s_i(n)]$, $H(K) = \text{DFT}[h(n)]$, $W_i(K) = \text{DFT}[w_i(n)]$ with variance, $\sigma_W^2 = N\sigma_n^2$, and $\text{DFT}[\cdot]$ stands for discrete Fourier transform (DFT) operation.

By applying zero-forcing frequency-domain equalization (FDE), the estimates of $C(K)$, $B(K)$, and $A(K)$ can be respectively expressed as

$$\begin{cases} \hat{C}(K) = \frac{Y_1(K)}{H(K)} = C(K) + \frac{W_1(K)}{H(K)} \\ \hat{B}(K) = \frac{Y_2(K)}{H(K)} = B(K) + \frac{W_2(K)}{H(K)} \\ \hat{A}(K) = \frac{Y_3(K)}{H(K)} = A(K) + \frac{W_3(K)}{H(K)} \end{cases} \tag{12}$$

where $A(K) = \text{DFT}[|a(n)|]$, $B(K) = \text{DFT}[|b(n)|]$, $C(K) = \text{DFT}[c(n)]$, $W_i(K)/H_i(K)$ is the noise component with the variance, $\sigma^2_{\tilde{W}_i(K)} = \sigma^2_W/|H_i(K)|^2$. Therefore, $|a(n)|$, $|b(n)|$, and $c(n)$ can be estimated as

$$\begin{cases} \hat{c}(n) = \text{IDFT}[\hat{C}(K)] = c(n) + \tilde{w}_1(n) \\ \widehat{|b(n)|} = \text{IDFT}[\hat{B}(K)] = |b(n)| + \tilde{w}_2(n) \\ \widehat{|a(n)|} = \text{IDFT}[\hat{A}(K)] = |a(n)| + \tilde{w}_3(n) \end{cases} \quad (13)$$

where $\text{IDFT}[\cdot]$ stands for inverse DFT (IDFT) operation, and $\tilde{w}_i(n) = \text{IDFT}[\frac{W_i(K)}{H(K)}]$.

Based on the estimate of $c(n)$, $\hat{c}(n)$, the polarity information can be demodulated. The estimates of $\text{sg}_{\text{Re}}(n)$ and $\text{sg}_{\text{Im}}(n)$ are assumed to be $\hat{\text{sg}}_{\text{Re}}(n)$ and $\hat{\text{sg}}_{\text{Im}}(n)$, respectively.

According to Eq. (5), the decoded polarity information, $\widehat{|a(n)|}$, and $\widehat{|b(n)|}$, the estimate of $x(n)$ is given by

$$\hat{x}(n) = \hat{\text{sg}}_{\text{Re}}(n)\widehat{|a(n)|} + j\hat{\text{sg}}_{\text{Im}}(n)\widehat{|b(n)|}. \quad (14)$$

After the N-point DFT, the estimated $X(K)$ can be derived as

$$\hat{X}(K) = \sum_{n=0}^{N-1} \hat{x}(n)e^{-j\frac{2\pi}{N}Kn} \quad K = 0, 1, \cdots, N-1. \quad (15)$$

Note that compared with the traditional optical OFDM, for example, DCO-OFDM, it is not easy to adopt bit or power loading in the proposed PIC-flip-OFDM because of the non-linear operation.

IV. COMPUTATIONAL COMPLEXITY

The computational complexity is defined as the number of DFT/IDFT operations at the transmitter or the receiver [6]. The comparison is given in Table II. The signal in the frequency domain does not need to be Hermitian symmetric in the proposed PIC-flip-OFDM, and the complexity of the transmitter in the proposed scheme is the lowest. Because FDE is employed to detect $A(K)$, $B(K)$, and $C(K)$, the computational complexity of the receiver of the proposed scheme is, although the highest, of the same order of magnitude as those of other schemes.

V. SIMULATION RESULTS

In the simulation, both the additive white Gaussian noise (AWGN) channel [8] and frequency selective channel [13] are considered. M-ary QAM (M-QAM) is used for all the modulated subcarriers, and the equal power allocation strategy is applied, that is, $\sigma^2_{X(K)} = \sigma^2_X$ ($K = 1, \cdots, N-1$, $K \neq N/2$), and $N = 512$. If the polarity information is decoded incorrectly, error will propagate. Eq. (14) shows that

TABLE II
COMPUTATIONAL COMPLEXITIES OF DIFFERENT SCHEMES

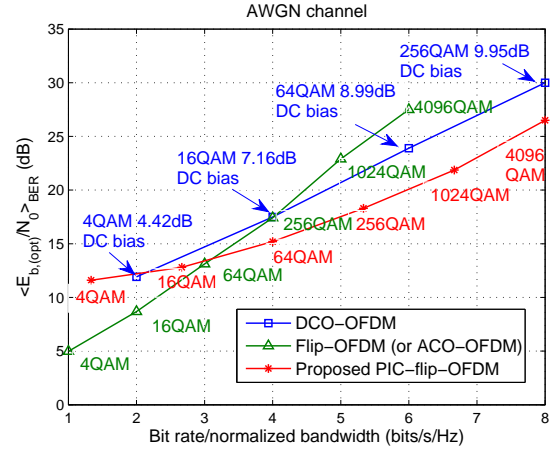|	Transmitter	Receiver
DCO-OFDM	$2N\log_2(N)$	$2N\log_2(N)$
ACO-OFDM	$4\frac{N}{2}\log_2(\frac{N}{2})$	$4N\log_2(N)$
Flip-OFDM	$2N\log_2(N)$	$2N\log_2(N)$
PIC-flip-OFDM	$N\log_2(N)$	$7N\log_2(N)$

Fig. 4. $< E_{b,(opt)}/N_0 >_{\text{BER}}$ versus bit rate/normalized bandwidth for different schemes in the AWGN channel.

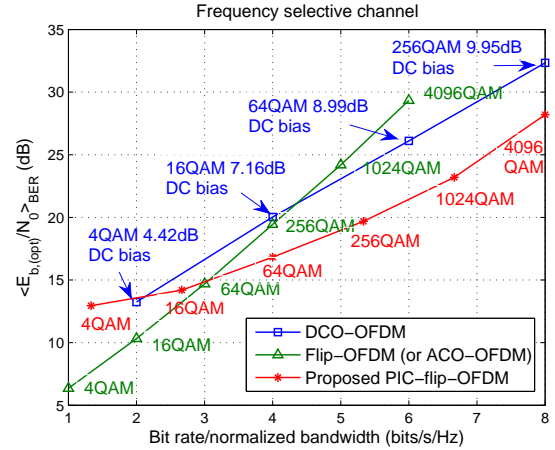Fig. 5. $< E_{b,(opt)}/N_0 >_{\text{BER}}$ versus bit rate/normalized bandwidth for different schemes in the frequency selective channel.

the detection performance of the proposed PIC-flip-OFDM depends on the decoded polarity information, $\widehat{|a(n)|}$, and $\widehat{|b(n)|}$. To minimize the bit error rate (BER), parameter κ is set as

$$\kappa = \frac{21\log_2(M)}{2(M-1)}. \quad (16)$$

The derivation of κ is given in the Appendix.

The optical energy per bit to single-sided noise power spectral density, $E_{b,(opt)}/N_0$, of the proposed PIC-flip-OFDM is [8], [11]

$$\frac{E_{b,(opt)}}{N_0} = \frac{(\mathbb{E}[s(n)])^2}{2BN_0} \cdot \frac{3N}{(N-2)\log_2(M)}. \quad (17)$$

Fig. 4 shows performances of different schemes in additive white Gaussian noise (AWGN) channel [8]. The required $E_{b,(opt)}/N_0$ for a BER of 10^{-3} [11], defined as $< E_{b,(opt)}/N_0 >_{\text{BER}}$, is used. Fig. 4 shows $< E_{b,(opt)}/N_0 >_{\text{BER}}$ against bit rate/normalized bandwidth for the proposed PIC-flip-OFDM, the traditional flip-OFDM, which can achieve the same power and spectral efficiencies as ACO-OFDM, and the DCO-OFDM with a DC bias [11], which is varied to achieve

the minimum $< E_{b,(opt)}/N_0 >_{\text{BER}}$ for different modulation orders through simulations. It can be seen from Fig. 4 that the optical power efficiency of the flip-OFDM is the highest when the bit rate/normalized bandwidth is less than 3 bit/s/Hz, that is the modulation order is low. However, the proposed PIC-flip-OFDM requires lower $< E_{b,(opt)}/N_0 >_{\text{BER}}$ than both the traditional flip-OFDM and the DCO-OFDM when the bit rate/normalized bandwidth is greater than 3.1 bits/s/Hz, which means that the proposed PIC-flip-OFDM can achieve the highest optical power efficiency. For example, 16-QAM DCO-OFDM, 64-QAM PIC-flip-OFDM, and 256-QAM traditional flip-OFDM achieve the same bit rate/normailzed bandwidth, that is, 4 bits/s/Hz. The $< E_{b,(opt)}/N_0 >_{\text{BER}}$ for the 64-QAM PIC-flip-OFDM is 15.1 dB, which is about 2 dB lower than what is required for 256-QAM traditional flip-OFDM and 16-QAM DCO-OFDM sent with a DC bias of 7.16 dB.

The performances of different schemes in the frequency selective channel is shown in Fig. 5. The channel with the parameters of configuration A in [13] is employed, and the used modulated bandwidth is $B = 100$ MHz. Therefore, the channel is frequency selective. In the simulation, the channel is slowly changing, and the impulse response of the channel is normalized as $\sum_n h_i(n) = 1$, the size of DFT is $N = 512$, and the length of CP is $N_g = 8$, which is greater than the delay spread of the channel. The required $< E_{b,(opt)}/N_0 >_{\text{BER}}$ in the frequency selective channel is higher than that in the AWGN channel for each OFDM scheme with the same bit rate/normalized bandwidth. Besides, almost the same conclusion can be derived as in Fig. 4. When the bit rate/normalized bandwidth is greater than 3 bits/s/Hz, the proposed PIC-flip-OFDM can achieve the highest optical power efficiency. The required $< E_{b,(opt)}/N_0 >_{\text{BER}}$ of the proposed PIC-flip-OFDM is about 3 dB and 5 dB less than that of the DCO-OFDM when the bit rate/normalized bandwidth is 4 bits/s/Hz and 8 bits/s/Hz, respectively.

VI. Conclusion

A new flip-OFDM named PIC-flip-OFDM scheme has been proposed in this letter. In this scheme, all subcarriers except the first and the middle ones can be data modulated, and consequently its spectral efficiency is improved when compared with the traditional flip-OFDM or ACO-OFDM scheme. The optical power efficiency of the proposed PIC-flip-OFDM scheme is higher than that of the DCO-OFDM scheme because the polarity information is coded. In addition, the proposed PIC-flip-OFDM can achieve the best performance when the bit rate/normalized bandwidth is greater than 3 bits/s/Hz, which is typically used in the optical communication systems.

Appendix

The derivation of κ

It is assumed that the bit error rate (BER) of $c(n)$ is $p_{e,1}$. When the polarity information is decoded correctly, the BER of $X(K)$ is assumed to be $p_{e,2}$. Therefore, the BER of the proposed scheme can be expressed as

$$P_e = 1 - (1 - p_{e,1})(1 - p_{e,2})$$
$$\approx p_{e,1} + p_{e,2}. \qquad (18)$$

To minimize the BER of the proposed scheme, κ is set to ensure that $p_{e,1}$ and $p_{e,1}$ decay on the same scale.

In the AWGN channel, the SER of the polarity information employing unipolar 4-PAM can be expressed as [9]

$$\text{SER}_{\text{U}-4-\text{PAM}} = \frac{2(4-1)}{4} Q\left(\sqrt{\frac{\sigma_c^2}{14\sigma_n^2}}\right)$$
$$= \frac{3}{2} Q\left(\sqrt{\frac{\kappa\sigma_x^2}{14\sigma_n^2}}\right). \qquad (19)$$

We consider high signal-to-noise ratio region, and the BER of the polarity information decays like [12]

$$p_{e,1} \sim \frac{1}{\log_2(4)} \frac{14\sigma_n^2}{\kappa\sigma_x^2}. \qquad (20)$$

When the polarity information is decoded correctly, according to Eq. (14), the BER of proposed scheme scales like [12]

$$p_{e,2} \sim \frac{1}{\log_2(M)} \frac{2(M-1)\sigma_n^2}{3\sigma_x^2}. \qquad (21)$$

Therefore, we set

$$\frac{1}{\log_2(4)} \frac{14\sigma_n^2}{\kappa\sigma_x^2} = \frac{1}{\log_2(M)} \frac{2(M-1)\sigma_n^2}{3\sigma_x^2}, \qquad (22)$$

and κ can be derived as

$$\kappa = \frac{21\log_2(M)}{2(M-1)}. \qquad (23)$$

References

[1] H. Zhu, and J. Wang, "Chunk-based resource allocation in OFDMA systems - Part I: chunk allocation," *IEEE Trans. Commun.*, vol. 57, no. 9, pp. 2734-2744, Oct. 2009.
[2] H. Zhu, and J. Wang, "Chunk-based resource allocation in OFDMA systems - Part II: joint chunk, power and bit allocation, *IEEE Trans. Commun.*, vol. 60, no. 2, pp. 499-509, Feb. 2012.
[3] O. Gonzalez, R. Perez-Jimenez, S. Rodriguez, J. Rabadan, and A. Ayala, "Adaptive OFDM system for communications over the indoor wireless optical channel," *IEE Proc. Optoelectronics*, vol. 153, no. 4, pp. 139-144, Aug. 2006.
[4] J. Armstrong, and A. Lowery, "Power efficient optical OFDM," *Ele. Lett.*, vol. 42, no. 6, pp. 370-371, Mar. 2006.
[5] S. Lee, S. Randel, F. Breyer, and A. Koonen, "PAM-DMT for intensity-modulated and direct-detection optical communication systems," *IEEE Photonics Technol. Lett.*, vol. 21, no. 23, pp. 1749-1751, Dec. 2009.
[6] N. Fernando, H. Yi, and E.Viterbo, "Flip-OFDM for unipolar communication systems," *IEEE Trans. Commun.*, vol. 60, no. 12, pp. 3726-3733, Dec. 2012.
[7] L. Wu, Z. Zhang, and H. Liu, "MIMO-OFDM visible light communications system with low complexity," in *Proc. IEEE Int. Conf. Commun.*, Budapest, Hungary, June 2013, pp. 2526-2530.
[8] J. Armstrong and B. J. C. Schmidt, "Comparison of asymmetrically clipped optical OFDM and DC-biased optical OFDM in AWGN," *IEEE Commun. Lett.*, vol. 12, no.5, pp. 343-345, May 2008.
[9] J. Barry, 'wireless infrared communications,' *Kluwer Academic publishers*, 1994.
[10] J. Proakis, 'Digital Communications,' 4th ed. *New York: McGraw-Hill*, 2001.
[11] S. D. Dissanayake, and J. Armstrong, "Comparison of ACO-OFDM, DCO-OFDM and ADO-OFDM in IM/DD Systems," *IEEE/OSA J. Light. Tech.*, vol. 31, no. 7, pp. 1063-1072, Apr. 2013.
[12] D. Tse and P. Viswanath, Fundamentals of wireless communication, Cambridge University Press, 2005
[13] J. R. Barry, J. M. Kahn, and et al, "Simulation of multipath impulse response for indoor wireless optical channels, *IEEE J. Sel. Areas Commun.*, vol. 11, no. 3, pp. 367-379, Apr. 1993.